Contents lists available at ScienceDirect

Journal of Organometallic Chemistry

journal homepage: www.elsevier.com/locate/jorganchem

Synthesis of dinitrosyl iron complexes (DNICs) with intramolecular hydrogen bonding

Show-Jen Chiou *, Chien-Chu Wang, Chih-Ming Chang

Department of Applied Chemistry, National Chiayi University, No. 300 Syuefu Road, Chiayi 600, Taiwan

ARTICLE INFO

ABSTRACT

$HSCH_2CONHCH_3$ and $HSCH_2CON(CH_3)_2$ containing a peptide bond are prepared for the synthesis of DNICs with/without intra-molecular hydrogen bonding, respectively. The IR $v(NO)$ bands of $[(NO)_2Fe(SCH_2CONHCH_3)_2]^-$ (2) appears at 1751, 1700 cm^{-1}. In complex 2, the presence of intramolecular [NH···S] hydrogen bonding was verified by the observation of IR spectroscopy with N–H stretching frequency 3334 cm^{-1} (CDCl$_3$) and subsequently confirmed by single-crystal X-ray diffraction showing N–S distance of 2.94 Å. Complex 2 displays the rhombic EPR spectrum with $g_1 = 2.039$, $g_2 = 2.031$ and $g_3 = 2.013$ at in frozen H$_2$O. Complexes 2 and 3 rapidly release NO when exposed to light. The time needed for photolysis reactions of 2 is two times faster than that of 3 in less polar solvent. Representative time courses for the photolability of 2 and 3 in THF display the NO-off ability: 2 > 3.

© 2008 Elsevier B.V. All rights reserved.

1. Introduction

Nitric oxide (NO) is one of the most important small molecules in physiology [1–3]. It is produced in a variety of mammalian cells by nitric oxide synthases (NOSs). As described as a "double-edged sword", it acts as critical endogenous regulator of blood flow, aggregation of platelet and a neurotransmitter at physiological levels (nano-molar); however, at higher levels (micro-molar), it is cytotoxic. Dinitrosyliron complexes (DNICs) and S-nitrosothiols (RSNOs) have been claimed as NO carriers that prolong its lifetime and preserve its biological activities for physiological functions. DNICs are classified into two categories, low-molecular-weight and protein-bound DNICs. LMW-DNICs are further classified by their electronic structures as EPR-active $[L_2Fe(NO)_2]^9$, EPR-silent $[L'_2Fe(NO)]^{10}$ (L = thiolate, L' = neutral ligands) and dimeric EPR silent/-active DNICs [4–6]. Li et al. reported the X-ray structure of DNIC with 1-methylimidazoles showing the diagnostic EPR signal of DNICs, $g = 2.03$ [4–7]. Darensbourg et al. employed N_2S_2 ligands mimicking the Cys–X–Cys motif to show that Fe(NO)$_2$ acts as an unit bound by different thiolate ligands [8]. Recently, Liaw and coworkers synthesized a series of LMW DNICs, $[S_5Fe(NO)_2]^-$ and $[(SR)_2Fe(NO)_2]^-$ (SR = thiolates) and showed the NO-releasing ability of DNICs modulated by the coordinated thiolates [9–13]. In addition to the NO-releasing ability regulation afforded by the coordinated ligands, the effect of hydrogen bonding commonly found in biology may further tune NO release. To probe the effect of hydrogen bonding in this regard, in this paper we report the syn-thesis, structure and characterization of $[PPN][(NO)_2Fe(SCH_2CONHCH_3)_2]$ (2) and $[PPN][((NO)_2Fe(SCH_2CON(CH_3)_2]$ (3). Structural and spectroscopic data establish that the former complex contains an intramolecular N–H···S bond. We have concluded that the NO-release ability of DNICs is significantly regulated by the intramolecular hydrogen bonding.

2. Experimental

All reagents were purchased from commercial sources and used as received, unless otherwise noted. Solvents were distilled under N$_2$ and dried as indicated. THF and hexanes were freshly distilled over Na/benzophenone, diethyl ether over CaH$_2$, acetonitrile over CaH$_2$/P$_2$O$_5$, methylene chloride over CaH$_2$ and methanol from Mg/I$_2$. N-methylmercaptoacetamide [14,15] and N,N-dimethyl mercaptoacetamide [14,15] were prepared as described previously. GSH-DNICs (GSH = Glutathione) was prepared using the previously reported methods [16]. Manipulations involving organometallic reagents were performed under a nitrogen atmosphere on a Schlenk line. Infrared spectra of the v_{NO} stretching frequencies were recorded on a Perkin–Elmer model spectrum One B spectrometer with sealed solution cells (0.1 mm, KBr windows). UV–Vis were recorded on a Cintra 202 spectrometer. The collected data were analyzed by Excel/Origin program. Analyses of carbon, hydrogen, and nitrogen were obtained with a CHN analyzer (Heraeus). Photolysis reactions were carried out in a 50 mL, water-cooled quartz reactor equipped with 16 mercury arc 8-W UV lamps (352 nm) outside the reactor. EPR spectra were recorded at X-band (9.5 GHz) by using a Bruker X-band E500CW spectrometer. The experiments at 77 K, the sample temperature was

* Corresponding author. Tel.: +886 963428025; fax: +886 52717901.
E-mail address: genechiou@mail.ncyu.edu.tw (S.-J. Chiou).

maintained at –196 °C by immersion of the EPR sample tube into a liquid nitrogen finger Dewar. Typical EPR measurement conditions were as follows: microwave frequency, 9.5 GHz; microwave power, 2 mW; modulation frequency, 100 kHz; modulation amplitude, 0.5 mT; receiver gain, 6.32×10^3.

Caution. N-methylmercaptoacetamide and *N,N*-dimethyl mercaptoacetamide are flammable liquids that present a pungent odour. The deprotonation reaction should be vented through an aqueous solution of NaOCl and NaOH.

2.1. Preparation of [PPN][SCH₂CONH(CH₃)]

NaSCH₂CONHCH₃ (70 mg, 0.55 mmol) and PPNCl (287 mg, 0.5 mmol) were dissolved in 25 mL MeOH and refluxed for 4.5 h. The solvent was removed under reduced pressure. The resulting residue was dissolved in CH₃CN. After stirring for 1 h, the solution was filtered and the solvent removed under reduced pressure. The resulting white solid was purified by recrystallization from CH₃CN/ Et₂O. Yield: 75%. ^{1}H NMR (DMSO-d^6) δ 2.54 (CH₃, d), 2.85 (CH₂, s), 7.72 ~ 7.53 (PPN, m), 8.88 (N*H*, b).

2.2. Preparation of [PPN][SCH₂CON(CH₃)₂]

NaSCH₂CON(CH₃)₂ (78 mg, 0.55 mmol) and PPNCl (287 mg, 0.5 mmol) were dissolved in 25 mL MeOH and refluxed for 4.5 h. The solvent was removed under reduced pressure. The resulting mixtures were dissolved in CH₃CN. After stirring for 1 h, the solution was filtered and the solvent removed under reduced pressure. The resulting white solid was purified by recrystallization from CH₃CN/Et₂O. Yield: 75%. ^{1}H NMR (DMSO-d^6) δ 2.65 (CH₃, s), 2.74 (CH₂, s), 3.12(CH₃, s), 7.72 ~ 7.53 (PPN, m).

2.3. Preparation of [(NO)₂Fe(SCH₂CONH(CH₃))₂Fe(NO)₂] (1)

[PPN][Fe(CO)₃(NO)] (355 mg, 0.5 mmol) and NOBF₄ (140 mg, 1.2 mmol) were combined in 25 mL THF at 0 °C and stirred for 15 min. The filtrate was added into a 10 mL THF solution of the thiol [PPN][SCH₂CONH(CH₃)] (643 mg, 1 mmol). After stirring for 1 h, the solution was filtered and the solvent was removed under reduced pressure. The resulting black–brown solid was purified by recrystallization from THF/Et₂O. Yield: 268 mg (61%). IR (THF): v/cm^{-1} = 1810(w, NO), 1778(vs, NO), 1750(vs, NO), 1686(s, CO). UV–Vis (THF) nm (ε, M^{-1} cm^{-1}): 218(58 505), 312(3634), 359(9596), 750(31). Anal. Calc. for C₆H₁₂Fe₂N₆O₆S₂: C, 16.38; H, 2.75; N, 19.10. Found: C, 16.25; H, 3.05; N, 18.85%.

2.4. Preparation of [PPN][(NO)₂Fe(SCH₂CONHCH₃)₂] (2)

[(NO)₂Fe(SCH₂CONH(CH₃))₂Fe(NO)₂] (91.2 mg, 0.2 mmol) and [PPN][SCH₂CONHCH₃] (257 mg, 0.4 mmol) were combined in THF (25 mL). After stirring for 30 min, the solution was filtered and the solvent was removed under reduced pressure. The resulting red brown solid was purified by recrystallization from THF/Et₂O/

hexane. Yield: 131 mg (76%). IR (THF): v/cm^{-1} = 1743(s, NO), 1693(vs, NO), 1666(s, CO). UV–Vis (THF) nm (ε, M^{-1} cm^{-1}): 267 (13 809), 367 (3286), 429 (1393), 768 (209). Anal. Calc. for C₄₂H₄₂FeN₅O₄P₂S₂: C, 58.40; H, 4.90; N, 8.07. Found: C, 57.82; H, 5.45; N, 7.72%.

2.5. Preparation of [PPN][(NO)₂Fe(SCH₂CON(CH₃)₂)₂] (3)

[(NO)₂Fe(SCH₂CON(CH₃)₂)₂Fe(NO)₂] (70 mg, 0.15 mmol) and [PPN][SCH₂CON(CH₃)₂] (202 mg, 0.31 mmol) were combined in THF (25 mL). After stirring for 30 min, the solution was filtered and the solvent was removed under reduced pressure. The resulting red brown solid was purified by recrystallization from THF/ Et₂O/hexane. Yield: 160 mg (60.4%). FTIR (THF) 1730(s), 1686(vs) cm^{-1} (vNO), 1642(s) cm^{-1} (vCO). UV–Vis (THF) nm (ε, M^{-1} cm^{-1}): 267 (17 191), 368 (3440), 429 (1067), 801 (223). Anal. Calc. for C₄₄H₄₆FeN₅O₄ P₂S₂: C, 59.33; H, 5.20; N, 7.86. Found: C, 59.95; H, 5.16; N, 7.26%.

2.6. Crystallographic structural determinations

Crystal data collection and refinement parameters are given in Table 2. Table 3 shows the atomic coordinates of complexes **1a** and **2b′**. Typically, the crystals were removed from the vial with a small amount of mother liquor and immediately coated with silicon grease on a weighing paper. A suitable crystal was mounted on a glass fiber with silicone grease and placed in the cold stream of a Bruker APEX II with graphite-monochromated Mo Kα radiation (λ = 0.71073 Å) at 150(2) K.

3. Results and discussion

To mimic small peptide with cysteine residues and to establish the desired intra/inter molecular hydrogen bonding within the iron complexes, *N*-methylmercaptoacetamide was synthesized by reaction of ethyl 2-mercaptoacetate and methylamine [14–15]. Reaction of Fe(CO)₂(NO)₂ and *N*-methylmercaptoacetamide yields the Roussin's red ester (RRE) [(NO)₂Fe(SCH₂CONH(CH₃))₂Fe(NO)₂] (**1**) (Scheme 1a) characterized by IR and UV–Vis spectroscopies. The dinuclear complex **1** exhibits diagnostic IR bands at v(NO) = 1810 (w), 1778 (vs), 1750 (vs) and v(CO) = 1686 (s) cm^{-1} with Δv(NO) = 28 cm^{-1} (the separation of 1778 and 1750 cm^{-1}) in THF. Consistent with RRE [(NO)₂Fe(SC₆H₄NHCOPh)₂Fe(NO)₂] displaying (v(NO) = 1816 (w), 1787 (vs), 1759 (vs) and v(CO) = 1686 (s) cm^{-1} (THF), complex **1** is described as a {Fe(NO)₂}^{9}–{Fe(NO)₂}^{9} coupled dimer, As such it is diamagnetic, no EPR signal is observed [11].

Cleavage of the thiolate bridges in **1** by addition of 2 equiv. of [PPN][SCH₂CONHCH₃] led to the formation of the dinitrosyliron complex [PPN][(NO)₂Fe(SCH₂CONHCH₃)₂] (**2**) (Scheme 1b) [12]. Alternatively, oxidation of Fe(CO)₂(NO)₂ by NOBF₄ followed by addition of [PPN][SCH₂CONHCH₃] also yielded complex **2** (Scheme 1c). Presumably, [NO]$^+$ oxidation of {Fe(NO)₂}^{10} Fe(CO)₂(NO)₂ yields the {Fe(NO)₂}^{9} [Fe(CO)₂(NO)₂]$^+$ intermediate [7], with subse-
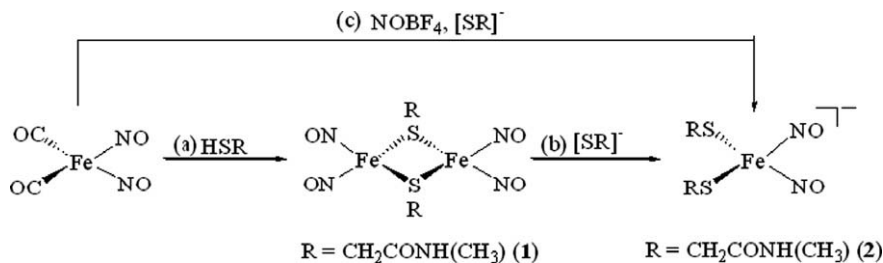
Scheme 1.

quent ligand-substitution between [PPN][SCH₂CONHCH₃] and [Fe(CO)₂(NO)₂]⁺ producing complex **2**. Brown red crystals of **2** exhibit IR absorptions at 1740, 1695, (ν(NO)) and 1664 (ν(CO)) cm⁻¹ and UV–Vis spectrum shows three intense absorption bands at 367, 417, 747 nm in THF. EPR spectrum of complex **2** displays an isotropic EPR signal at $g = 2.028$ at 298 K and the rhombic signal with $g_1 = 2.039$, $g_2 = 2.029$ and $g_3 = 2.014$ at 77 K in THF. Complex **2** displays a rhombic signal with $g_1 = 2.039$, $g_2 = 2.031$ and $g_3 = 2.013$ in frozen (and degassed) H₂O (Fig. 3), consistent with that of GSH-DNICs (GSH = Glutathione) [16]. Complex **2** is stable in the degassed and deionized water. It is noted that the water-solubility of anionic {Fe(NO)₂}⁹ DNICs is reportedly limited thus, related biological studies of complex **2** are ongoing in our laboratory. The single-crystal X-ray structure of complex **2** (Fig. 1) shows the coordination sphere of Fe is pseudo tetrahedral based on the N–Fe–N and S–Fe–S bond angles of 117.0° and 110.4°, respectively. The average Fe–N(O) and N–O bond distances of complex **2** are 1.665(3) Å and 1.187(3) Å, respectively. Average Fe–N(O) bond distance falls in the range of 1.695(3)–1.661(6) Å and the average N–O bond distance is within the range of 1.178(3)–1.160(6) which is corresponding to the characteristics of mononuclear {Fe(NO)₂}⁹ DNICs [9,13].

The average Fe–S bond lengths and IR stretching frequencies of several thiolate ligated DNICs are listed in Table 1. The mean value of the Fe–S bond lengths in complexes **2**, [PPN][(2-S-(C₄H₃S)₂Fe(NO)₂], [PPN][(SC₆H₄-o-NHCOCH₃)₂Fe(NO)₂] and [PPN][(SEt)₂Fe(NO)₂] are 2.292(1), 2.296(1), 2.301(1) and 2.275(2), respectively. The average Fe–S bond length of complex **2**, longer than that of [PPN][(SEt)₂Fe(NO)₂], is presumably attributed to the intramolecular [N–H...S] interaction (N···S distance of 2.9721(26) Å in complex **2**) (Fig. 1) [17–19]. The N···S distance as short as 2.97 Å has been observed in bent NH···S hydrogen bonds such as those in o-amino thiolate [20–22]. Zuppiroli et al. [23,24] have studied HSCH₂CONHCH₃ with IR in CCl₄ and the results show the ligand favored the cyclization as a five membered ring including the proton on nitrogen. In the solid state, HSCH₂CONHCH₃ shows a tendency to form the interligand N–H···O hydrogen bond, e.g. as found in Hg(SR)₂ (SR = SCH₂CONHCH₃). The X-ray structure of Mo[BH-(Me₂pz)₃](NO)(SR)₂ (SR = SCH₂CONHCH₃) synthesized by Walter et al. shows the existence of both an intramolecular hydrogen bond
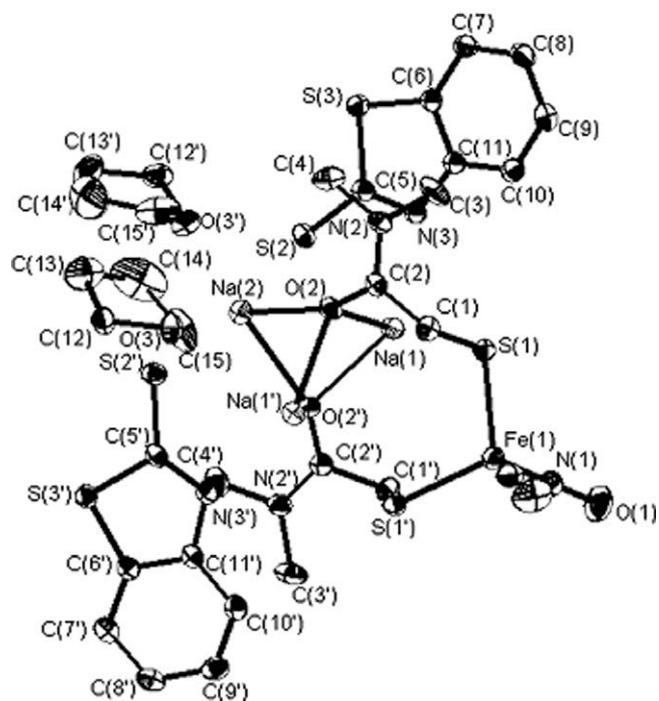

Fig. 2. ORTEP drawing and labeling scheme of {[Na][(NO)₂Fe(SCH₂CON(CH₃)₂)]} · 2{[Na][SC₇H₄SN]} (**3′·2{[Na][SC₇H₄SN]}**). Selected bond distances (Å) and angles (°): Fe(1)–N(1) 1.6870(15); Fe(1)–S(1) 2.2998(5); N(1)–O(1) 1.1715(19); N(3)–Na(1) 2.4597(15); Na(1)–O(2) 2.7014(13); Na(1)–S(1) 2.9454(8); Na(1)–S(2) 3.0131(8); Na(1)–Na(2) 3.2646(10); Na(2)–O(3) 2.3590(14); Na(2)–O(2) 2.5043(13); Na(2)–S(2) 2.9410(5); N(1)–Fe(1)–S(1) 112.76(5); O(1)–N(1)–Fe(1) 164.84(15); N(3)–Na(1)–O(2) 88.84(4); N(3)–Na(1)–S(1) 93.46(4); O(2)–Na(1)–S(1) 71.59(3); N(3)–Na(1)–S(2) 58.27(4); O(2)–Na(1)–S(2) 90.72(3); S(1)–Na(1)–S(2) 147.54(3); O(3)–Na(2)–O(2) 167.46(5); O(3)–Na(2)–S(2) 78.54(3); O(3)–Na(2)–S(2) 78.54(3).
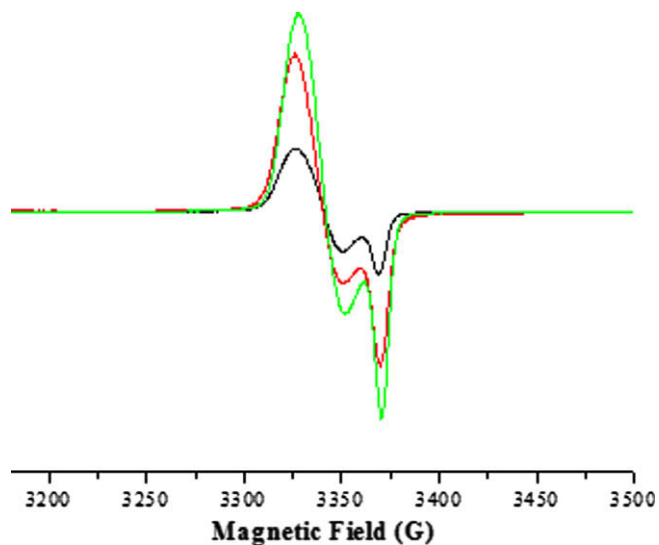

Fig. 3. EPR spectra of complexes **2**, **3**, and GSH-DNIC at frozen. (– : **2**;   : GSH-DNIC;   : **3**)

Fig. 1. ORTEP drawing and labeling scheme of [((NO)₂Fe(SCH₂CONHCH₃)₂]⁻ (**2**). Selected bond distances (Å) and angles (°): Fe(1)–N(1) 1.661(3); Fe(1)–N(2) 1.670(3); Fe(1)–S(1) 2.2745(10); Fe(1)–S(2) 2.3093(10); N(1)–O(1) 1.182(3); N(2)–O(2) 1.192(3); N(1)–Fe(1)–N(2) 116.99(13); N(1)–Fe(1)–S(1) 110.37(9); S(1)–Fe(1)–S(2) 110.39(4); O(1)–N(1)–Fe(1) 168.7(3); O(2)–N(2)–Fe(1) 68.2(2).

N–H···S and an intermolecular hydrogen bond N–H···O; furthermore, the N–H···O linkage is likely disrupted in solution [14–15]. Herein, the structure of complex **2** reveals only an intramolecular hydrogen bond N–H···S supported by the single IR ν(NH) at 3334 cm⁻¹ in CDCl₃ corresponding to the hydrogen-bonded N–H group [14–15]. The remarkable solubility of **2** in water may be attributed to the hydrogen bond acceptor ability of the carbonyl of amide group.
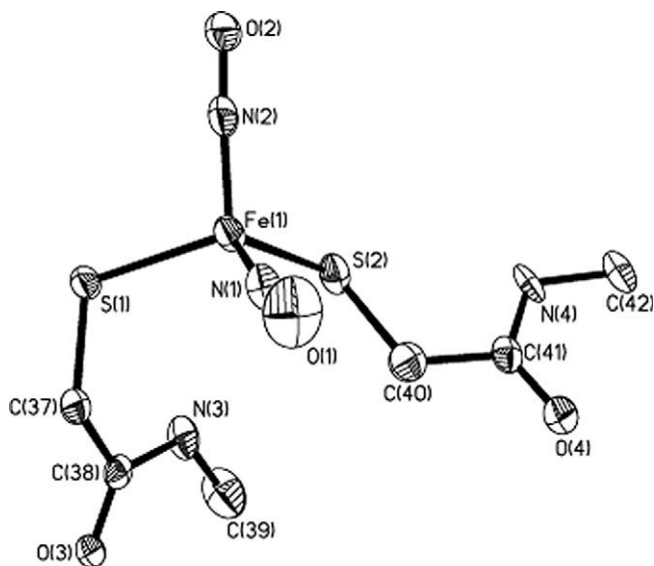
Table 1
Selected Fe–S bond lengths and IR stretching frequencies for the anionic thiolate ligated $\{Fe(NO)_2\}^9$ DNICs

Anionic thiolate ligated $\{Fe(NO)_2\}^9$ DNICs	ν_{NO} (cm^{-1}, THF)	$\Delta\nu_{NO}$ (cm^{-1})	Fe–S (Å)	Reference
2	1740, 1695	45	2.292(1)	This work
3	1730, 1686	44	–	This work
[PPN][(2-S-(C$_4$H$_3$S)$_2$Fe(NO)$_2$]	1743, 1698	45	2.296(1)	[10]
[PPN][(SC$_6$H$_4$-o-NHCOCH$_3$)$_2$Fe(NO)$_2$]	1752, 1705	47	2.301(1)	[10]
[PPN][(SEt)$_2$Fe(NO)$_2$]	1715, 1674	51	2.275(2)	[17]

Table 2
Selected IR stretching frequencies of complex **2**, **2′**, **3** and **3′** in THF

Complexes	cm^{-1}
2	1740(s), 1695(vs), 1664(s), 1589(w)
2′	1744(s), 1697(vs), 1663(b)
3	1730(s), 1686(vs), 1642(s), 1589(w)
3′	1742(s), 1698(vs), 1637(b)

Table 3
Time required for photolysis reactions

Complex	CH$_2$Cl$_2$[a]	THF[a]	CH$_3$CN[a]	DMSO[b]
2	180(±5)	210(±4)	210(±6)	180(±4)
3	300(±5)	300(±5)	210(±5)	180(±4)
3′	180(±6)	210(±7)	150(±7)	180(±3)

[a] Determined by FTIR.
[b] Determined by UV–Vis (unit: minute).

In contrast to the existence of intramolecular [N–H···S] hydrogen bonding observed in complex **2**, the dinitrosyl complex [PPN][(NO)$_2$Fe(SCH$_2$CON(CH$_3$)$_2$)$_2$] (**3**) with no hydrogen-bonding capacity was synthesized. As reported by Liaw and coworkers, ligand-substitution reaction occurred upon addition of the stronger nucleophile ([SR′]$^-$, R′ = SC$_6$H$_4$-o-NHCOCH$_3$, Ph or 2-S-C$_4$H$_3$S) into THF solution of [PPN][(NO)$_2$Fe(SC$_7$H$_4$SN)$_2$] leading to the formation of complex [PPN][(NO)$_2$Fe(SR′)$_2$] [9–13]. Complex **3** was isolated either from reaction of [PPN][(NO)$_2$Fe(SC$_7$H$_4$SN)$_2$] and [PPN][SCH$_2$CON(CH$_3$)$_2$] (N,N-dimethylmercapto-acetamide was obtained from reaction of ethyl 2-mercaptoacetate and dimethyl-amine) [14–15] in THF or the reaction as synthesis of complex **1** via RRE, [(NO)$_2$Fe(SCH$_2$CON(CH$_3$)$_2$)$_2$Fe(NO)$_2$] (**4**) and [PPN][SCH$_2$CON(CH$_3$)$_2$]. The ESI MS spectrum shows a *M* peak at 352 *m/z* which clearly indicates complex **3** with the stoichiometry as [PPN][(NO)$_2$Fe(SCH$_2$CO N(CH$_3$)$_2$)$_2$]. The present of NO group is also supported by the appearance of the peak at 322 (*M*–NO). The IR stretching frequencies of complex **3** appear at ν(NO) = 1730 (vs), 1686 (vs) and ν(CO) = 1642 (w) cm^{-1}. The IR stretching frequencies of complexes **2**, **2′**, **3** and **3′** are summarized in Table 2. The IR ν(NO) of complex **3** shifting by 10 cm^{-1}, in comparison with that of complex **2**, indicates the intramolecular hydrogen bonding in **2** decreases the electron back donation from iron dπ to NO π^* orbitals. Interestingly, the EPR spectrum of complex **3** displays an isotropic EPR signal at g = 2.027 at 298 K and a rhombic signal with g$_1$ = 2.041, g$_2$ = 2.032 and g$_3$ = 2.012 at 77 K in THF. The EPR spectrum of complex **3** displays a rhombic signal with g$_1$ = 2.039, g$_2$ = 2.031 and g$_3$ = 2.013 in frozen (degassed) H$_2$O. These results are similar to complex **2** and GSH-DNIC (Fig. 3). In addition, reaction of [PPN][(NO)$_2$Fe(SC$_7$H$_4$SN)$_2$] and [Na][SCH$_2$CON(CH$_3$)$_2$] in THF solution at ambient temperature resulted in the formation of [Na][(NO)$_2$Fe(SCH$_2$CON(CH$_3$)$_2$)$_2$] (**3′**).
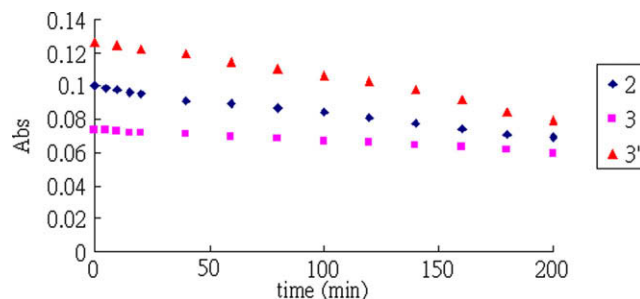
Fig. 4. Continuous monitoring the decay of absorbance values at 768, 801, and 775 nm of **2** (♦), **3** (■) and **3′** (▲), respectively, in THF at 25 °C. The concentration of complexes **2**, **3** and **3′** is 6.25×10^{-4} M.

Fig. 2 displays single-crystal X-ray structure of complex **3′** co-crystallized with two thiolates [Na][SC$_7$H$_4$SN] and two THF molecules. The interactions of Na$^+$ and the donor atoms, O, S, and N, in complex **3′** may serve to stabilize the structure. The cation exchange reaction from [PPN]$^+$ to [Na]$^+$ was conducted to synthesized complex **2′**.

In the dark, both **2** and **3** are stable for weeks in the solid state and solutions of CH$_2$Cl$_2$, THF and CH$_3$CN. However, when exposed to visible light, both complexes decompose gradually. Besides the insoluble black powder, the IR spectrum show there is no band of NO but the carbonyl group of thiolate in solution. To compare the photolability of the bound NO, the photolysis reactions of complexes **2** and **3** were conducted in CH$_2$Cl$_2$, THF and CH$_3$CN and DMSO. All reactions were monitored by FTIR and UV–Vis spectrometry. The times needed for the reactions to reach completion are collected in Table 3. Complex **2** releases NO in the less polar solvents CH$_2$Cl$_2$ and THF about 2.5 times faster than **3**. Furthermore, the reaction times are similar in more polar solvents, i.e. CH$_3$CN and DMSO. These results suggest a role for the intramolecular hydrogen bonding in **2** may enhance NO release in the less polar solvents and as the effect of hydrogen bond is diminished in polar solvents, the rates of NO release become similar. For complex **3**, the NO release seems to be dominated by solvent effects as well. In addition, based on the structure of **3′**, the cation, Na$^+$ is sustained by S and O from ligands. The Na$^+$ shares the electron density on S and makes the time needed for NO release as faster as **2**.

Another experiment to elucidate the effect of hydrogen bonding and cation Na$^+$ is the photodecomposition reactions monitored by UV–vis spectrometry. Representative time courses for the photolability of **2**, **3** and **3′** in THF are shown in Fig. 4. It displays the NO-off ability: **2** ≈ **3′** > **3** (The slope of **2** ≈ **3′** is 20×10^{-5} and 7.0×10^{-5} for **3**). The result is resembled to those reported by Liaw et al. [10]; the less electron-donating, coordinated thiolate ligands, the better NO-donor ability.

4. Conclusions

The water soluble complex [PPN][(NO)$_2$Fe(SCH$_2$CONHCH$_3$)$_2$] (**2**) with intramolecular hydrogen bonding and [PPN][(NO)$_2$Fe(SCH$_2$CON(CH$_3$)$_2$)$_2$] (**3**) were synthesized. The [N–H···S] intramolecular interaction in complex **2** was characterized by means of IR spectroscopy and single-crystal X-ray diffraction. Complexes **2** and **3** exhibit rhombic EPR signal with g$_{av}$ = 2.03, the characteristic of GSH-DNIC in biological system. The notable water solubility of **2** and **3** may be caused by the intermolecular hydrogen bonds between these complexes and water. Both complexes are photolabile and rapidly release NO upon illumination with visible or UV light. The more efficient NO-releasing ability of complex **2**, compared to that of complex **3**, is attributed to the existence of [N–H···S] intramolecular hydrogen bonding. The cation Na$^+$ also

plays the similar role to affect NO release. The results here imply that protein-bound DNICs preserve the sensitive $\{Fe(NO)_2\}^9$ core in a hydrophobic environment and employ hydrogen bonding to further tune the condition of NO release. On the other hand, Na^+, an essential ion in biological system, may have a similar influence as hydrogen bonding while a hydrophilic environment dominates.

Acknowledgements

Appendix A. Supplementary material

Supplementary material associated with this article can be found, in the online version, at doi:10.1016/j.jorganchem. 2008.08.034.

References

[1] D.E. Koshland, Science 258 (1992) 1861.
[2] G.R. May, P. Crook, P.K. Moore, C.P. Page, Br. J. Pharmacol. 102 (1991) 759.
[3] Yp. Tao, T.P. Misko, A.C. Howlette, C. Klein, Development 124 (1997) 3587.
[4] A.J. Vithayathil, J.L. Temberg, B. Commoner, Nature 207 (1965) 1246.
[5] M.W. Foster, J.A. Cowan, J. Am. Chem. Soc. 121 (1999) 4093.
[6] C.E. Cooper, Biochim. Biophys. Acta 1411 (1999) 290.
[7] N. Reginato, C.T.C. McCrory, D. Pervitsky, L. Li, J. Am. Chem. Soc. 121 (1999) 10217.
[8] C-Y. Chiang, M.L. Miller, J.H. Reibenspies, M.Y. Darensbourg, J. Am. Chem. Soc. 126 (2004) 10867.
[9] M.L. Tsai, C.C. Chen, I.J. Hsu, S.C. Ke, C.H. Hsieh, K.A. Chiang, G.H. Lee, Y. Wang, J.M. Chen, J.F. Lee, W.F. Liaw, Inorg. Chem. 43 (2004) 5159.
[10] F.T. Tsai, S.J. Chiou, M.C. Tsai, M.L. Tsai, H.W. Huang, M.H. Chiang, W.F. Liaw, Inorg. Chem. 44 (2005) 5872.
[11] M.-L. Tsai, W.-F. Liaw, Inorg. Chem. 45 (2006) 6583.
[12] M.-L. Tsai, C.-H. Hsieh, W.-F. Liaw, Inorg. Chem. 46 (2007) 5110.
[13] M.-C. Hung, M.-C. Tsai, G.-H. Lee, W.-F. Liaw, Inorg. Chem. 45 (2006) 6041–6047.
[14] J. Huang, R.L. Ostrander, A.L. Rheingold, Y. Leung, M.A. Walters, J. Am. Chem. Soc. 116 (1994) 6769.
[15] J. Huang, R.L. Ostrander, A.L. Rheingold, Y. Leung, M.A. Walters, Inorg. Chem. 34 (1995) 1090.
[16] A.F. Vanin, V.P. Mokh, V.A. Serezhenkov, E.I. Chazov, Nitric Oxide 16 (2007) 322–330.
[17] T.-T. Lu, S.-J. Chiou, C.-Y. Chen, W.-F. Liaw, Inorg. Chem. 45 (2006) 8799–8806.
[18] T. Okamira, S. Takmizawa, N. Ueyama, A. Nakamura, Inorg. Chem. 37 (1998) 18–28.
[19] S.J. Chiou, C.G. Riordan, A.L. Rheingold, PNAS 100 (2003) 3695–3700.
[20] J. Huang, J.C. Dewan, M.A. Walters, Inorg. Chim. Acta 228 (1995) 199–206.
[21] N. Ueyama, T.A. Okamura, A.J. Nakamura, J. Chem. Soc. Chem. Commun. (1992) 1019–1020.
[22] T.a. Okamura, N. Ueyama, A. Nakamura, E.W. Ainscough, A.M. Brodie, J.M. Walters, J. Chem. Soc. Chem. Commun. (1992) 1658–1660.
[23] G. Zuppiroli, C. Perchard, M.H. Baron, C. de Loze, J. Mol. Struct. 69 (1980) 1–16.
[24] C. Perchard, G. Zuppiroli, P. Gouzerh, Y. Jeannin, F. Robert, J. Mol. Struct. 72 (1981) 119–129.